energies

Article

Comparative Analysis of XLPE and Thermoplastic Insulation-Based HVDC Power Cables

Jae-In Lee, Woo-Hee Jeong, Minh-Chau Dinh, In-Keun Yu and Minwon Park *

Department of Electrical Engineering, Changwon National University, Changwon 51140, Republic of Korea
* Correspondence: capta.paper@gmail.com; Tel.: +82-55-213-3638

Abstract: The application of cross-linked polyethylene (XLPE) cables to voltage sourced converter (VSC)-based high voltage direct current (HVDC) systems has already been technically verified and has become common, and thermoplastic (TP) is attracting attention as an insulation material for next-generation cables due to the recent development of material-related technologies. However, studies related to TP cables are mainly focused on improving material properties, and studies related to cable systems are insufficient. In this paper, XLPE and TP cables were designed for application to VSC-based HVDC systems, and major characteristics such as electric field distribution and thermal stability were compared and analyzed through overvoltage simulation. The insulation design method of HVDC cable was presented, and the design was performed using XLPE and TP insulation materials. The temperature and electric field profiles of the cables were also analyzed through a finite element method simulation. To analyze the performance of the designed cable, it was simulated with the PSCAD/EMTDC program. Based on the simulation results, the major characteristics of XLPE and TP cables were compared and analyzed. Results showed that in the case of TP cables, insulation properties were excellent, but thermal conductivity was relatively low; therefore, countermeasures are needed.

Keywords: HVDC cable design; HVDC cable electric field distribution; HVDC cable FEM simulation; HVDC cable insulation design; HVDC cable recommended test; overvoltage of HVDC cable

Citation: Lee, J.-I.; Jeong, W.-H.; Dinh, M.-C.; Yu, I.-K.; Park, M. Comparative Analysis of XLPE and Thermoplastic Insulation-Based HVDC Power Cables. *Energies* **2023**, *16*, 167. https://doi.org/10.3390/en16010167

Academic Editors: Yalin Wang, Shihang Wang and Jiaming Yang

Received: 5 December 2022
Revised: 16 December 2022
Accepted: 20 December 2022
Published: 23 December 2022

1. Introduction

Compared with the conventional line-commutated converter (LCC) based high voltage direct current (HVDC) system, the voltage sourced converter (VSC) based HVDC system has many technical and economic advantages, such as the converter station's footprint, operational flexibility, and independent control of active and reactive power [1–4]. In particular, it has a large advantage over competing technologies in renewable energy and cross-border power grid connection projects, due to technological advantages such as black start and switching of power direction without voltage reversal [5–7]. The VSC-based HVDC system overcomes the high voltage limit with the introduction of modular multi-level converter (MMC) technology and reduces harmonics and conversion losses occurring in the switching stage [8]. Since the first commercialization of the MMC-HVDC system through the Trans Bay Cable project in 2010, the MMC-HVDC system has secured a significant share in the HVDC market, which is ongoing [9,10]. This trend has caused changes not only in HVDC converters but also in the cable market. HVDC systems based on VSC (including MMC) have boosted the introduction of DC cables with extruded insulation, since VSC technology enables the reversal of power flow direction without inversion of voltage polarity [11].

A variety of HVDC cable technologies have been developed over the past few decades and are operating successfully. Most HVDC cables installed to date are based on paper/oil or mass-impregnated insulation systems, but due to manufacturing complexity and low operating temperature limitations, interest is shifting towards polymeric insulation-based cables [12,13]. Early in the process of introducing VSC-HVDC, extruded polymer insulation (cross-linked polyethylene: XLPE) cable was also introduced. For extruded cables, the rated power and voltage gradually increased from the 80 kV class. However, in recent years, companies such as ABB and NKT have competitively announced the development of HVDC XLPE cable technology and commercialized it in various projects [14,15]. Currently, XLPE cables of over 600 kV are being produced. As XLPE technology rises to a stable commercial level, research on HVDC extruded cables is moving on to next-generation cables that will go beyond the technical limits of XLPE. Thermoplastic (TP) is the most studied material for the next-generation insulator of HVDC cables. Compared with conventional XLPE insulators, TP insulator does not generate crosslinking byproducts and have excellent electrical and mechanical properties due to the high breaking strength, flexibility, and temperature resistance of the insulator [16–19]. In addition, since the TP insulator can be recycled after its lifespan, it is economically and environmentally superior [20]. For this reason, various cable developers are developing TP cables, but only Prysmian has succeeded in commercializing them [21].

Cables with TP insulation are not the only advantages over XLPE. The TP insulator has lower thermal conductivity compared to XLPE, so even if the same current flows through the conductor, the thermal emissivity to the surroundings is lower than XLPE, and the internal temperature increases higher [22]. Therefore, the temperature difference between the inside and outside of the insulator increases, which affects the conductor resistance increase and electric field distribution. Insulator thickness selection in consideration of electric field distribution due to insulator temperature difference is one of the key factors in insulator design [23]. For this reason, research on TP insulators is focused on improving the material performance of insulators or on the CIGRE recommended test. Extruded HVDC cables generally must be evaluated against the various test items presented in CIGRE TB-852 before being sold on the market [24,25]. In many studies related to TP cables, the focus of electric field analysis is limited to electric field distribution through simulation or to achieving the recommended test parameters of CIGRE TB-852. However, when introducing a new system, it is necessary to anticipate possible problems through various analyses in addition to using existing evaluation methods.

Regarding XLPE cables for HVDC, various analyses have already been performed in connection with these studies. Ref. [26] conducted a study on the electrical behavior of XLPE used for HVDC cable insulation. Ref. [23] analyzed the thermal instability of XLPE cables based on CIGRE TB-496 (pre-revised version of TB-852) [27]. Ref. [28] performed a lifespan analysis based on the overvoltage phenomenon that occurred in XLPE cables. Ref. [29] analyzed the characteristics of overvoltage in relation to cable constants in HVDC systems to which XLPE cables are applied. On the other hand, research on TP cables remains in the pre-application stage for HVDC systems. Most of the research is conducted with the aim of improving and analyzing the properties of insulators [30–32]. Even for the TP cables independently developed by the leading group, Prysmian, only a review of the recommended test evaluation was performed [21]. In order to replace XLPE cables with TP cables, more research needs to be done on various aspects of the cables. In particular, as with XLPE, the TP cable's field strength, temperature, and allowable ampacity analyses must be performed, not only for the tests recommended by CIGRE-852 but also for the transient operating environments such as overvoltages.

In this paper, XLPE and TP cables used in the MMC-HVDC system were modeled, and the characteristics under various voltage conditions were compared and analyzed. The direction of improvement of the HVDC power cable based on TP insulation was discussed based on the comparative analysis results. A method for designing and verifying cable insulation was presented. A case study was conducted by applying XLPE and TP insulators according to the studied method. For the case study, a ±250 kV, 1 kA/pole, 100 km symmetrical monopole MMC HVDC system using only underground cables was selected as the target. The general properties of XLPE and TP insulation materials were investigated to design cables suitable for the target system. Cable design was performed based on the investigated insulation materials. The designed cables were analyzed for temperature and electric field distribution through finite element method (FEM) simulations utilizing COMSOL Multiphysics. In addition, by applying the designed cable, the overvoltage that can be experienced in the MMC-HVDC was analyzed through PSCAD/EMTDC simulation and the electric field was calculated during the transient state.

As a result, in the proposed system, the TP cable can maintain the required insulation performance with a thinner insulation thickness based on higher insulation performance than XLPE. With these advantages, it is economical, and it is possible to manufacture stable cables against transient overvoltage. In addition, it was confirmed that despite the higher thermal resistance, the maximum allowable temperature was high, so that a larger current could flow. However, since the low thermal conductivity of TP insulator shows a large difference in electric field distribution as the insulator radius increases, improving the thermal conductivity of TP cable is a problem to be solved first for commercialization. It is certain that these research results can be used as basic data for performance evaluation and design process improvement of TP cables for HVDC in the future.

2. Design of Extruded Cables for HVDC System Power Transmission

2.1. Extruded HVDC Cable Insulation and Design Methods

XLPE material is widely used as an insulation material for HVDC cables. However, the operating temperature of HVDC cable with XLPE insulation material is limited to 70 °C, making it difficult to increase the capacity of the transmission system [26]. The XLPE has a complicated manufacturing process, a high likelihood of defects due to crosslinking by-products generated during the manufacturing process, and it is vulnerable to partial discharge. In addition, it can easily induce space charge accumulation under high DC electric field stress, which can shorten cable life [25]. From an environmental point of view, XLPE is a thermosetting polymer, so it cannot be recycled, and it causes environmental problems and economic costs in the disposal process [33]. In order to overcome the disadvantages of XLPE, research on alternative TP polymers continues. Among the TP materials, the most representative material is polypropylene (PP). PP is expected to be an insulating material for next-generation HVDC cables because it has characteristics such as excellent insulation performance, high operating temperature, chemical resistance, and recyclability [16–20].

In this paper, in order to compare and analyze the characteristics of cables using XLPE and PP materials, the design was performed using pure XLPE and PP materials, and the characteristics were confirmed under load cycle tests and overvoltage stress. Insulator design only considers the thermal and electrical properties of the insulator. Mechanical properties such as stiffness and bending stress and chemical properties are not covered. Figure 1 shows the design and verification processes for the HVDC cable insulation performed in this paper.

First, the voltage, capacity, and usage environment of the target HVDC system should be reviewed. The cross-sectional area of the conductor appropriate for the design goal is selected (actually, the current capacity according to the temperature of the insulator should be designed as in ref. [34], but since this paper only deals with the insulator design, it is replaced by the nominal cross-section). The most important factor in cable insulation design is to establish the design electrical stress of insulation $E(d)$. The cable insulation must be designed so that its most stressed point can withstand an $E(d)$ for a design life. When setting $E(d)$, factors such as degradation of insulation performance must also be considered, so an electrical-statistical approach should be used [35,36]. $E(d)$ can be obtained through Equations (1)–(5). It starts by setting the DC withstand voltage U_{DC}, which can be expressed according to the traditional method as [11]:

$$U_{DC} = U_0 \cdot K_1 \cdot K_2 \cdot K_3 \tag{1}$$

where,

U_0 = HVDC rated voltage (pole-to-ground voltage)
K_1 = deterioration coefficient of insulator
K_2 = temperature coefficient of insulator
K_3 = safety factor for uncertainties

$$K_1 = \left(\frac{design\ life\ of\ a\ power\ cable}{time\ duration\ of\ DC\ test\ voltage}\right)^{1/n} \tag{2}$$

where, n is the life exponent ($10 \leq n$).

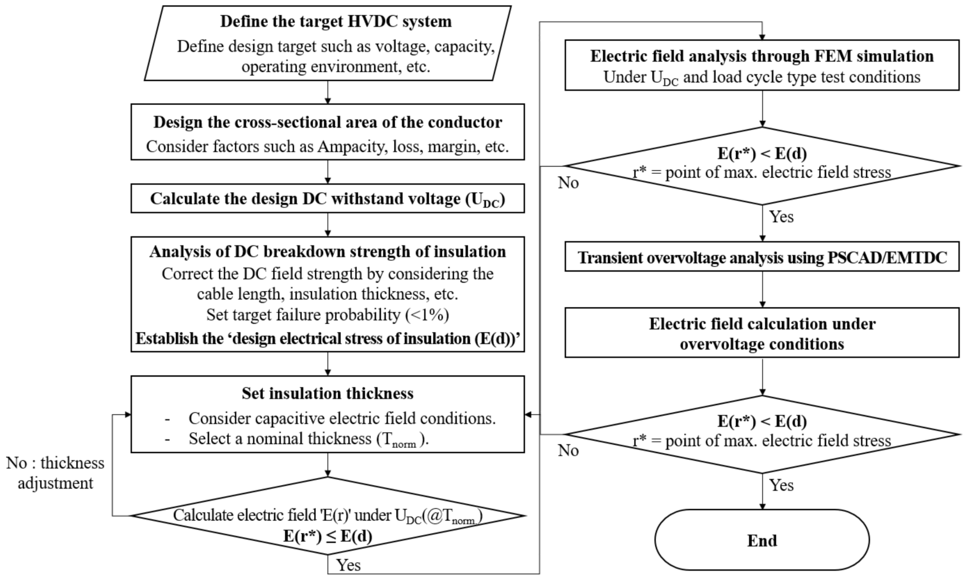

Figure 1. Design and verification processes for an HVDC cable insulation.

According to Equation (1), U_{DC} represents the withstand voltage considering insulator performance degradation during its lifetime. In general, the withstand level of an insulator is based on the higher U_{DC} or the maximum impulse withstand level. However, in this paper, since the maximum impulse withstand level is reviewed through simulation in a later step, the withstand level is set based on U_{DC} in the current step.

The next step is to confirm electrical properties such as DC breakdown strength and space charge stress modification of the insulation material. DC breakdown strength is expressed through a two-parameter Weibull distribution, and the probability of breakdown (P) in the electric field (E) is as shown in Equation (3).

$$P = 1 - \exp\left[-\left(\frac{E}{E_0}\right)^{\beta}\right] \tag{3}$$

where, E_0 is a scale parameter corresponding to a failure probability of 63.2%, and β is a shape parameter. The DC breakdown strength obtained from specimens or mini-cables is corrected for thickness and length through Equations (4) and (5).

$$E_t = \frac{E_0}{N^{1/\beta}} \tag{4}$$

$$E_l = \frac{E_t}{\left(\frac{l_2}{l_1}\right)^{1/\beta}} \tag{5}$$

where, E_t is a scale parameter that corrects the thickness, E_l is a scale parameter that corrects the length from E_t, N is the thickness ratio of the actual insulation to the specimen, and l_1 and l_2 are the lengths of the test cable (mini-cable) and actual cable, respectively. In general, the probability of failure due to DC breakdown strength is set to 1% or less. Finally, considering the modification margin of the electric field caused by the space charge at the breakdown strength corresponding to the set probability, $E(d)$ can be obtained. The next step is to calculate the minimum insulation thickness T_{min}; it is calculated based on the cable's capacitive electric field distribution and is obtained through Equation (6).

$$T_{min} = r_i \left[\exp\left(\frac{U_{DC}}{r_i \cdot E(d)} \right) - 1 \right] \quad (6)$$

where, r_i is the inner radius of the insulator. If a nominal insulation thickness (T_{min}) equal to or greater than the minimum insulation thickness is selected, the electric field distribution $E(r)$ is analyzed based on the capacitive field strength.

$$E(r) = \frac{U_{DC}}{r \ln(r_o / r_i)} \quad (7)$$

where, r_o is the outer radius of the insulator and r is the point between r_i and r_o. When r^* is the most stressed point ($r^* \in r$), $E(r^*) \leq E(d)$ must be satisfied. Otherwise, the insulation thickness must be properly adjusted.

The next step is to examine the insulation design by considering the electric field distribution due to the electrical conductivity of the cable insulation under DC stress. As will be discussed in detail in Section 2.2, HVDC electric field distribution is affected by electrical conductivity, unlike AC, so the electric field distribution changes from capacitive to resistive, and the electric field distribution can be reversed. Accordingly, it is necessary to check the electric field distribution considering the change in electrical conductivity of the cable insulation. At this time, $E(r^*) \leq E(d)$ must be satisfied in U_{DC} and load cycle type tests. The final step is to satisfy $E(r^*) \leq E(d)$ under the overvoltage conditions experienced when applied to the target HVDC system.

In order to compare and analyze the characteristics of cables with XLPE and PP insulators, a case study was conducted on cables for MMC-HVDC systems with a rated voltage of ±250 kV. It is assumed that the target HVDC system does not perform voltage reversal in operation. The properties of the insulator can be affected by factors such as the manufacturing process, thermal treatment, and additives. For this reason, in order to obtain reproducible general results, the insulation design was performed using pure XLPE and pure isotactic PP materials in this study. Cable insulation materials were investigated through various references, and materials close to the average were selected, excluding samples with extreme performance [37–52]. The parameters used for the insulation design are presented in Table 1. The Weibull distribution of the calibrated cable DC breakdown strength is shown in Figure 2.

Table 1. Insulation design parameters for ±250 kV HVDC cables.

Symbols	XLPE	PP	Symbols	XLPE	PP
U_0 (kV)	250	250	P (%)	1	1
U_{DC} (kV)	599	599	Operating Temp. (°C)	70	70
K_1	2.18	2.18	N	132	175
Design life (year)	40	40	E_t (kV/mm)	178.6	169.3
Time duration of DC test voltage (h)	3	3	E_l (kV/mm)	73.7	92.4
K_2	1	1	l_1 (m)	1	1
K_3	1.1	1.1	l_2 (m)	100,000	100,000
n	15	15	T_{min} (mm)	24.5	13.16
r_i (mm)	16.4	16.4	T_{norm} (mm)	25	14
r_o (mm)	41.4	30.4	Space charge modification (%)	30	15
E_0 (kV/mm)	260	222.2			
β	13	19	$E(d)$ (kV/mm)	40	63

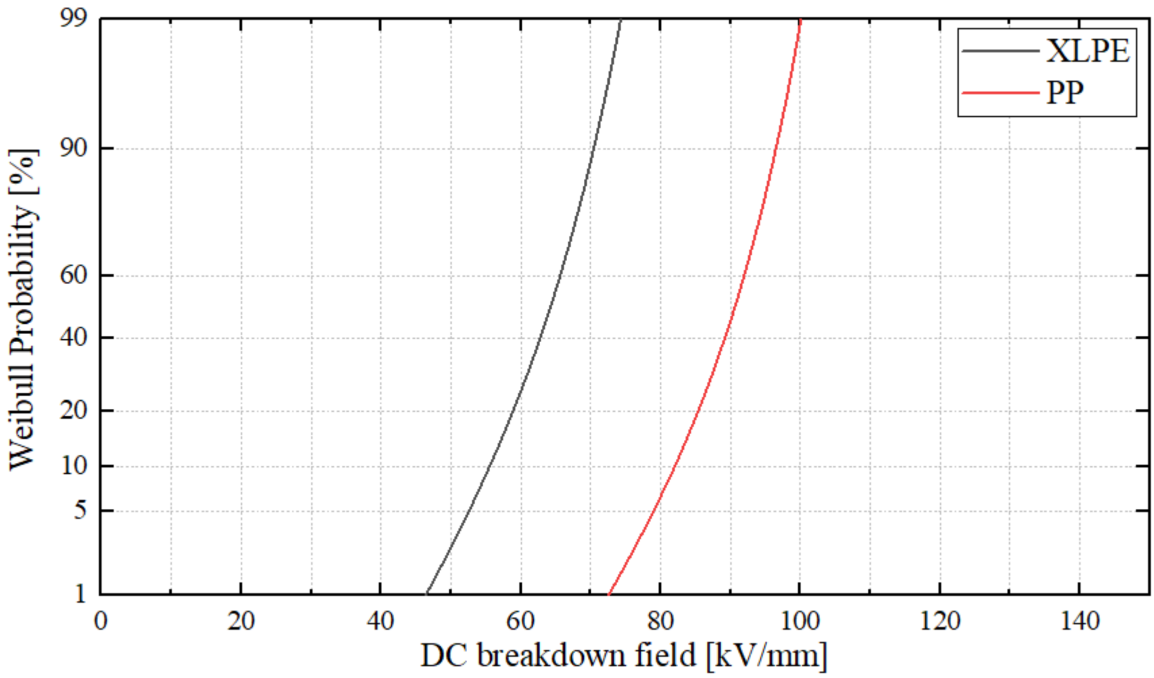

Figure 2. Weibull probability vs. DC breakdown field of the calibrated cables.

2.2. The Electric Field Characteristics of an HVDC Cable Insulation

Under AC stress, the electric field distribution within the cable insulation is determined by the permittivity of the insulation, and the variability is less than 1%, as it is not greatly affected by the surrounding environment such as operating conditions or temperature [35]. However, under DC stress, the electric field distribution within the cable insulation is affected by the conductivity as well as the permittivity of the insulation. Conductivity is greatly affected by temperature and field strength [53]. Since the conductivity of an insulator generally increases exponentially as the temperature increases, the conductivity value inside the insulator changes as shown in Equation (8) according to the temperature difference between the inside and the outside during cable operation.

$$\sigma(T, E) = \sigma_0 \exp[a(T - T_0) + b(E - E_0)] \tag{8}$$

where a and b are the temperature coefficient and electric field coefficient, respectively, related to the conductivity of the insulator.

Due to this change in conductivity, the conductivity of the conductor side, which has a relatively high temperature during cable operation, has a significantly higher value than the sheath side conductivity. As a result, an electric field reversal phenomenon in which the electric field strength at the conductor side is lower than the likely electric field strength at the sheath side. These differences must be considered in order to analyze the electric field distribution of a DC cable. Assuming that the HVDC cable insulation is homogeneous, the steady-state DC field $E_{DC}(r)$ can be obtained from the following equations, including the effects of temperature and field dependence [11,54,55]:

$$E_{DC}(r) = \frac{\delta U_0 (r/r_o)^{\delta-1}}{r_o\left[1 - (r_i/r_o)^{\delta}\right]} \tag{9}$$

$$\delta = \left[\frac{a\Delta T}{\ln(r_o/r_i)} + \frac{bU_{DC}}{(r_o - r_i)}\right] / \left[1 + \frac{bU_{DC}}{(r_o - r_i)}\right] \tag{10}$$

where, δ is the field reversal coefficient and ΔT is the temperature drop across the insulation thickness. δ increases with cable current, and if $\delta > 1$, an electric field reversal occurs in the insulation wall of the HVDC cable when the load increases. The highest electric field is found in the inner insulator when $\delta < 1$ and in the outer insulator when $\delta > 1$.

As mentioned, Equation (9) is a relational expression representing the electric field distribution for the steady state of the cable. In order to analyze the electric field distribution inside the insulator of a DC cable in a transient state such as a fault, it is necessary to understand the target of application of the above formulas. This understanding starts with the dielectric time constant τ. For the dielectric time constant τ is commonly used for DC extruded cables, and 10 τ is a value considering sufficient stability. 10 τ depends on the temperature, but even if a conservative value is applied at a temperature of 90 °C, it has a value of more than 200 s [24]. The overvoltage phenomenon to be considered in this paper is a short time overvoltage phenomenon of less than 100 ms. The instantaneous voltage change occurring at this time can be assumed as a situation in which a change value is added in a steady state without disturbing the electric field in the existing electric field distribution. Therefore, the electric field appearing in the transient state can be expressed as Equation (11).

$$E_{transient}(r,t) = E_{DC}(r) + E_{AC}(r,t) \tag{11}$$

$$E_{AC}(r,t) = \frac{U(t) - U_0}{r \ln(r_o/r_i)} \tag{12}$$

where $U(t)$ is the magnitude of the voltage over time in the transient state.

2.3. Cable Modeling for FEM Simulation

For performance comparison between cables, HVDC cables using XLPE and PP insulators were designed according to the design process described in Section 2.1. Nominal values were applied in the same way for all other configurations except for the cable insulation. The shape of the cable is presented in Figure 3, and the structural dimensions of each layer of the cable are shown in Table 2.

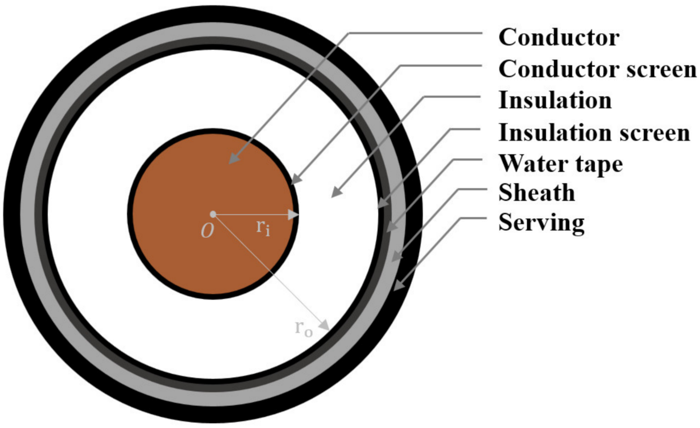

Figure 3. Structure of the extruded cable.

Table 2. Structural dimensions according to cable insulation materials.

Items	Materials	XLPE Cable	PP Cable
Radius of the conductor (mm)	Copper	14.9	14.9
Thickness of the conductor screen (mm)	Sem i-conducting PE	1.5	1.5
Thickness of the insulation (mm)	XLPE or PP	25	14
Thickness of the insulation screen (mm)	Semi-conducting PE	1.5	1.5
Thickness of the water tape (mm)	PVC (Poly vinyl chloride)	1.5	1.5
Thickness of the sheath (mm)	Aluminum	3	3
Thickness of the serving (mm)	PVC	4.5	4.5
Total radius of the cable (mm)	-	51.9	40.9
Burial depth (mm)	Soil	1.5	1.5
Distance between each pole (mm)	-	300	300

The material properties of the cables used in the FEM simulation are shown in Table 3, and some data values in Table 3 change with temperature.

Table 3. Material properties of the cables applied in FEM simulation (@ Room temperature).

Materials	Specific Heat Capacity [J/kg·K]	Density [kg/m^3]	Thermal Conductivity [W/m·K]	Relative Permittivity ε_r	Electrical Conductivity [S/m]
Copper	383	8938	402	1	5.95×10^7
Semi-conducting PE	2405	1055	0.286	2.25	0.002
XLPE	2302	930	0.328	2.5	1) *
PP	1900	900	0.224	2.2	2) *
Aluminum	897	2699	237	1	3.65×10^7
PVC	1080	1574	0.15	-	-
Soil	800	1515	1.3	-	-

1) * The electrical conductivity of XLPE is calculated by Equation (8): $\sigma_0 = 3 \times 10^{-16}$ [S/m], a = 0.084, b = 0.0645 [Refer to Figure 4a]. 2) * Refer to Figure 4b.

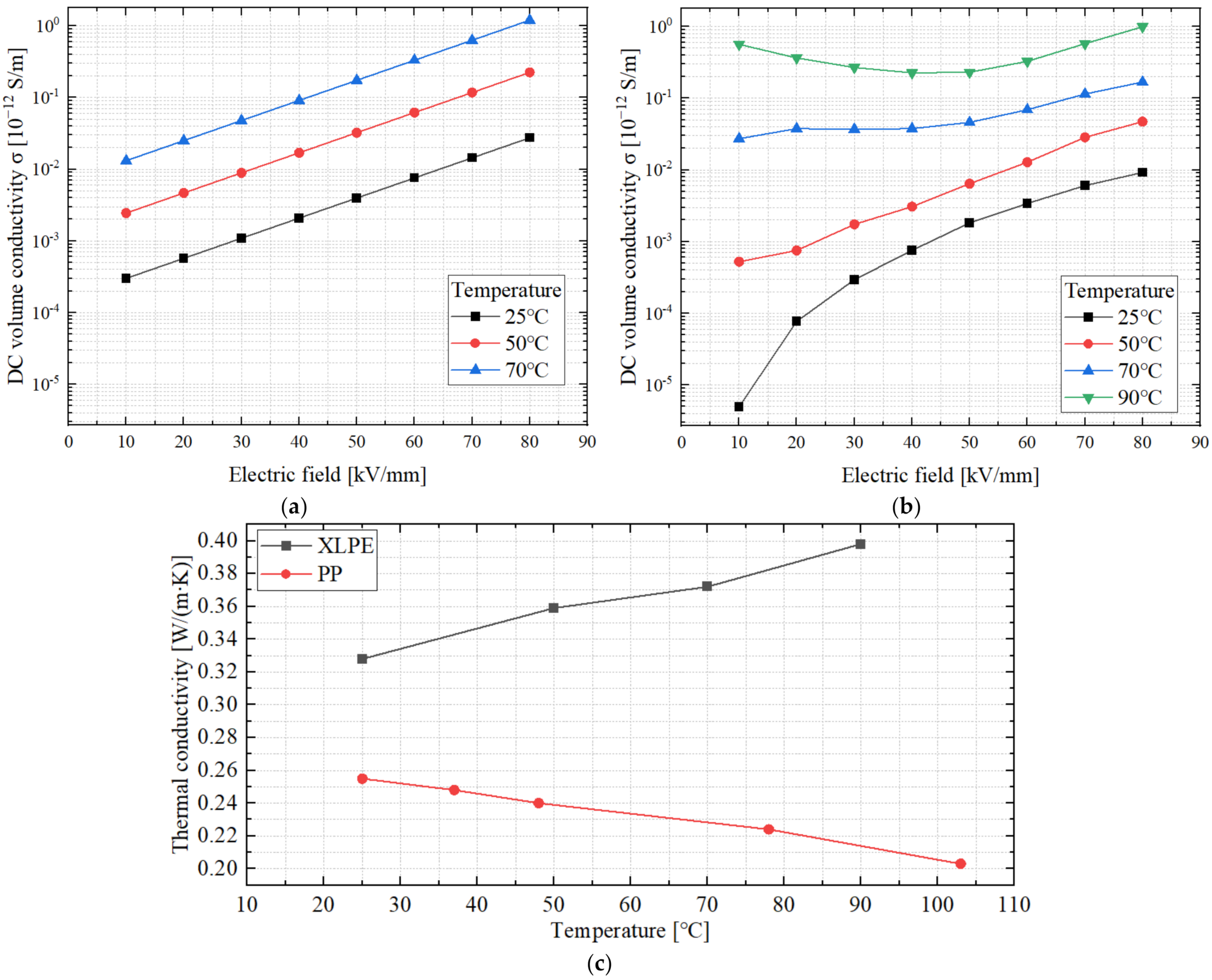

Figure 4. (**a**) DC volume conductivity of XLPE material; (**b**) DC volume conductivity of PP material; (**c**) Thermal conductivity of insulation versus temperature.

When analyzing electric field distribution of cable insulation under DC stress, the electrical conductivity is one of the most critical parameters. As can be seen from Equation (8), the conductivity is a value that changes depending on the temperature and the strength of the electric field. In the case of XLPE, whose characteristics have already been analyzed a lot, universal model parameters are provided for Equation (8). Figure 4a shows the conductivity of the XLPE insulation calculated through Equation (8) (see footnote in Table 3 for details). However, in the case of PP, there is no universal model for Equation (8) yet. Therefore, the conductivity of PP is calculated using an interpolation function based on the measured data used in the design, and the data used is shown in Figure 4b. Figure 4b shows the DC volume conductivity data measured while gradually increasing the electric field under four temperature conditions.

Thermal conductivity is also a parameter that has a major influence on the results. Compared to XLPE, PP has a lower thermal conductivity, and the thermal conductivity increases with increasing temperature for XLPE, while the thermal conductivity decreases for PP. In order to accurately reflect this, the change according to temperature was applied as shown in Figure 4c.

3. Cable Design Verification and Electric Field Analysis

3.1. Electric Field Analysis of Cable Insulations under Various Conditions

The cable modeled in Section 2.3 was analyzed through FEM simulation. FEM simulations were performed using COMSOL Multiphysics [56]. The cable model was analyzed for the following cases.

(a) Temperature profile of cable insulation;
(b) Electric field distribution under rated and load cycle type test (LCTT) voltage conditions;
(c) Electric field distribution at U_{DC} voltage;
(d) Electric field distribution under transient overvoltage conditions.

Regarding the temperature profile analyzed in case (a), the room temperature (25 °C) condition before heating is called the cold cable, and the operating temperature (70 °C) condition is called the hot cable. Cases (b)~(c) are analyzed under the cold cable and hot cable conditions, respectively.

(a) Temperature profile of cable insulation

The temperature distribution within the cable is analyzed by applying a 24-h load cycle according to CIGRE TB-496 [27]. The 24-h load cycle is broken down into three phases:

(1) 0–6 h: Heating the conductor from room temperature to the rated conductor temperature through the Joule heat of the conductor;
(2) 6–8 h: Maintaining the temperature above rated operating temperature;
(3) 8–24 h: Reducing the temperature back to room temperature through natural cooling.

The temperature profile of cable insulation during LCTT is shown in Figure 5a. Arc length in the figure represents the distance from the inside of the insulator to the outside (i.e., from the conductor screen surface to the insulator screen surface).

Based on 8 h, the temperature difference between the inside and outside of the cable insulation is 22.4 °C and 20.6 °C, and despite the high thermal resistance of the PP cable, the temperature difference between the inside and outside of the insulator is smaller because of its thinness. However, it shows a larger temperature difference based on the same distance from the center. Figure 5b shows the temperature distribution at the LCTT and when sufficient time is maintained until the temperature distribution is stabilized at the operating temperature. Afterwards, the hot cable (full load) condition stands for the stabilized state of the cable temperature distribution.

(b~c) Electric field distribution under various test voltages

Electric field distribution was analyzed for the rated voltage (U_0), LCTT voltage ($1.85U_0$), and DC withstand voltage U_{DC}. Analysis was performed for no load (the cold cable) and full load (the hot cable). The electric field distributions under the test voltages are shown in Figure 6.

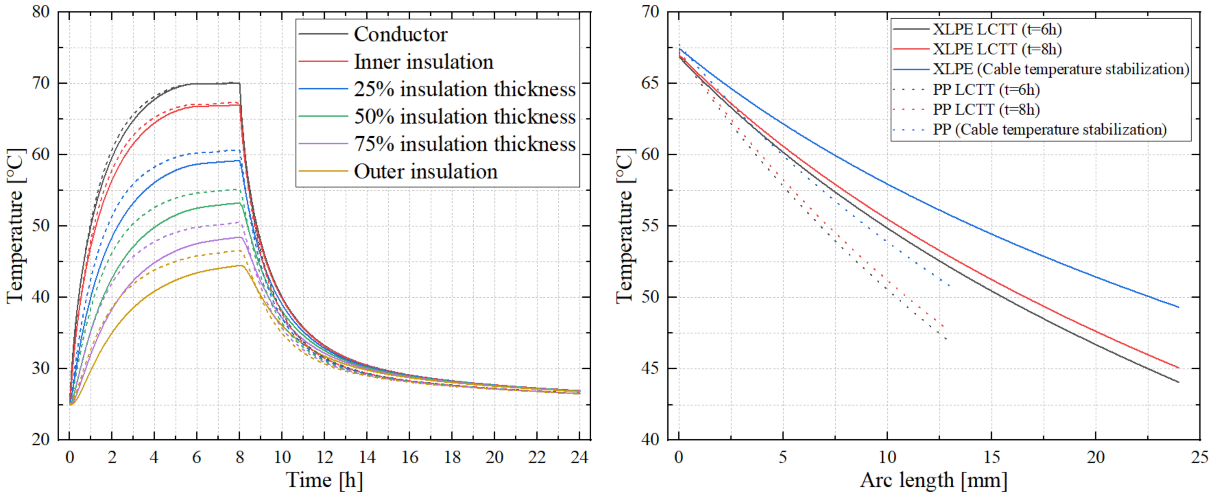

(a) (b)

Figure 5. (**a**) Cable insulation temperature profile during LCTT (Line: XLPE, Dot: PP); (**b**) Cable insulation temperature profile (Line: XLPE, Dot: PP).

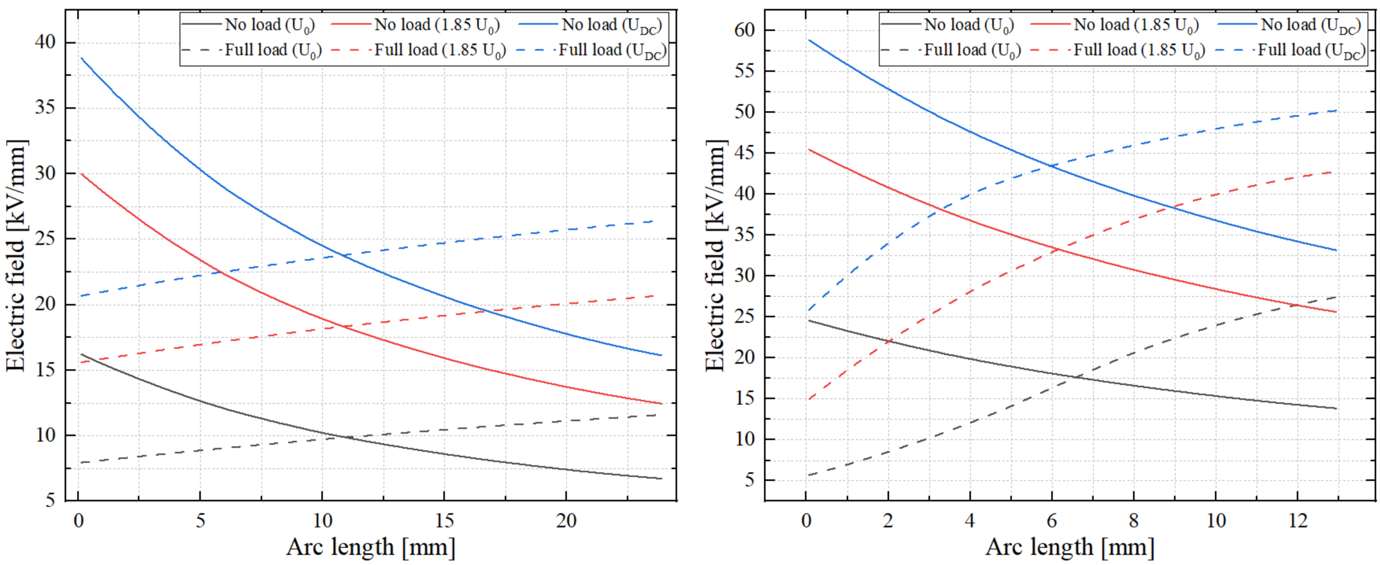

(a) (b)

Figure 6. Electric field profile of the cable insulation under various voltage conditions (**a**) XLPE cable; (**b**) PP cable.

As a result of the simulation, it was confirmed that the electric field reversal phenomenon appeared in both cables. However, it was confirmed that the design electrical stress of insulation $E(d)$ was not exceeded even under the highest U_{DC} condition, and the internal electric field of the cold cable under no load increased as the voltage level increased. The simulation results are summarized as shown in Table 4.

The possibility of increasing the capacity of PP cable for the same conductor cross-sectional area was analyzed by FEM simulation. Insulation temperature measurement for the current was performed after temperature stabilization across the cable. The temperature variations in Figure 7 are the values measured at the innermost part of the insulator (maximum temperature point).

Table 4. Comparative analysis of cable insulations.

Descriptions	XLPE	PP
Insulation thickness [mm]	25	14
ΔT between r_i and r_o [°C]	18.2	17
Average temperature difference [°C/mm]	0.73	1.21
Insulation loss (at full load, U_0) [mW/m]	0.287	0.207
Current at operating temperature (70 °C) [A]	1265	1215
Electric field difference between r_i and r_o (at full load, U_0) [kV/mm]	4.5	22.5

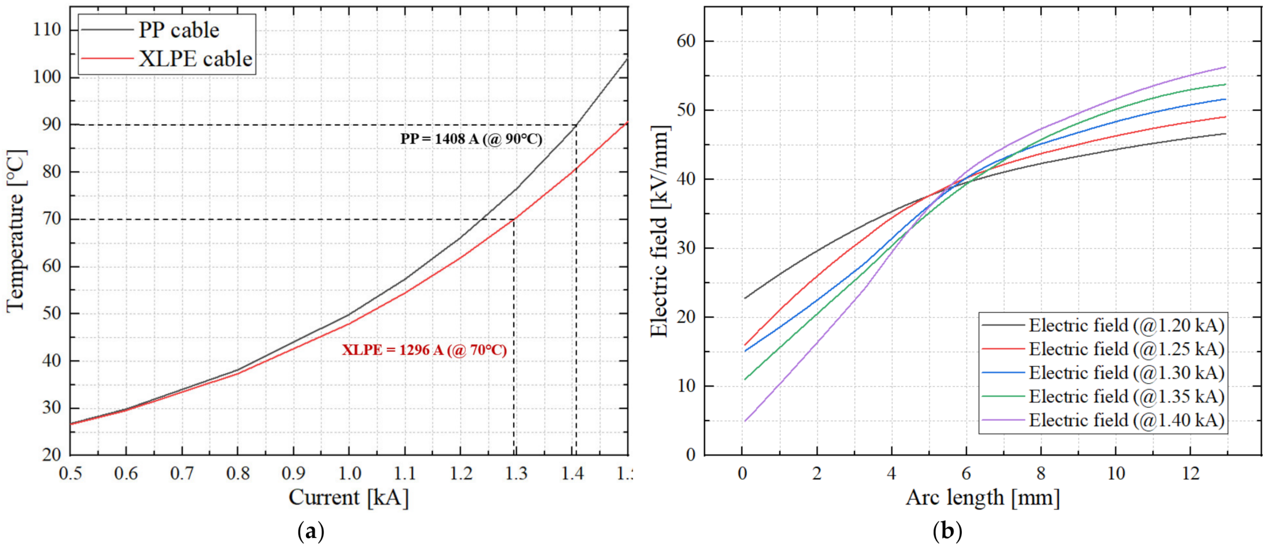

Figure 7. (**a**) Maximum temperatures of the XLPE and PP cable insulations with increasing currents; (**b**) electric field profiles of the PP cable by current variations (under U_{DC}).

In general, the operating temperature of XLPE is 70 °C, and in the case of PP insulator, there is no experience in DC systems yet, but it is known to be 90 °C. At the same temperature, an XLPE cable with higher thermal conductivity can carry a higher current. However, it can be seen that the ampacity increases by about 100 A (8%) in the conductor of the same cross-sectional area (630 mm^2), to 1296 A for XLPE and 1408 A for PP cable at the maximum operating temperature condition, respectively. The current limit due to the electric field was also reviewed, and it was confirmed that $E(r^*) \leq E(d)$ was satisfied at 1400 A.

3.2. Overvoltage Analysis of Cables Applied to HVDC Systems

The analysis of threatening overvoltages in cables of MMC-HVDC systems has been investigated in various papers and cases [24,57–61]. Even if the overvoltage of a cable has the same cause, the magnitude of the maximum overvoltage may vary depending on the configuration of the system. These differences can be overcome within the protection margins of the system but can sometimes cause damage to the system.

Among the various overvoltage phenomena that cables can experience in a cable-only transmission system, the most threatening overvoltage is the voltage superposition experienced by the connected electrode when a fault occurs in the DC line. In this paper, the overvoltage was analyzed in the HVDC system to which the designed cable was applied.

An MMC-HVDC system was modeled to analyze the overvoltages. The target system is MMC-HVDC with symmetrical monopolar topology, and the rated voltage and current are selected as ±250 kV and 1 kA/pole, respectively. The schematic diagram of the target system and the basic parameters of the system are shown in Figure 8 and Table 5, respectively.

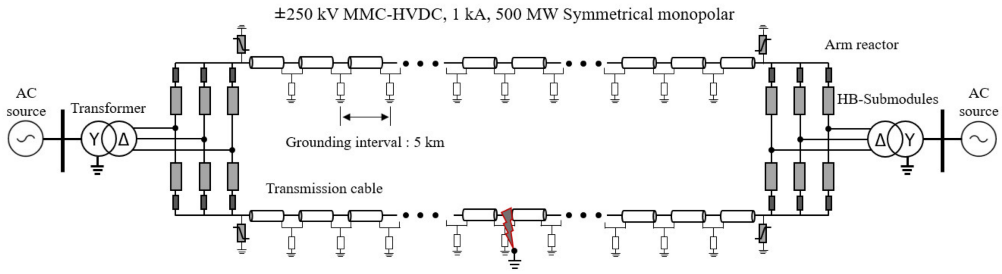

Figure 8. Schematic diagram of the MMC-HVDC system.

Table 5. Specifications of the MMC-HVDC system.

Descriptions	Values
Rated power	500 MW
Nominal DC voltage (pole-to-ground)	±250 kV
Nominal AC voltages (AC grid/Valve side)	154 kV/250 kV
AC short circuit ratio	10
AC system frequency	60 Hz
Number of submodules per arm	250
Average submodule voltage	2 kV
Capacitance of each submodule capacitor	6.5 mF
Protection level surge arrestor	1.8 p.u.

The overall modeling of the MMC-HVDC system was performed by referring to the CIGRE working group's "Guide for the Development of Models for HVDC Converters in an HVDC Grid" [62]. Both ends of the converter and cable are protected by surge arresters. A reactor installed on the converter arm is placed between the converter and the cable. As a control strategy, MMC 1 is driven through active/reactive power control, and MMC 2 is driven through DC voltage/reactive power control. The submodule was selected in the half-bridge method and implemented as an equivalent model corresponding to the type model 4 classified in Ref. [62]. The transmission distance is 100 km, and a frequency-dependent model is applied. Both ends of the cables are grounded with 10 Ω, and the cable sheath is grounded with a ground resistance of 0.1 Ω every 5 km. Cables were modeled using the parameters in Tables 2 and 3.

Through simulation using PSCAD/EMTDC [63], the transient overvoltage was analyzed for the voltage change of the opposite healthy electrode in the event of a single pole-to-ground fault, and the analysis results are shown in Figure 9.

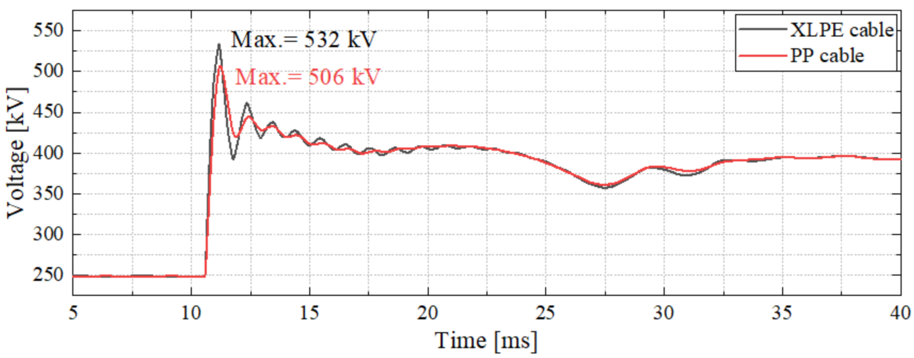

Figure 9. Overvoltage simulation results according to cable insulation.

As a result of the simulation, the overvoltages experienced by the XLPE and PP cables show similar waveforms, but there are differences in the maximum overvoltage and vibration damping. In the case of applying the XLPE cable under the same conditions, the maximum overvoltage is 532 kV, and the PP cable is 506 kV, showing a difference of

0.1 p.u. based on the rated voltage. This is caused by the difference in capacitance due to the thickness and permittivity of the insulator, and the capacitance is calculated by Equation (13) [29].

$$C_{cable} = 1000 \times 2\pi \times \varepsilon_0 \varepsilon_r / \ln(r_o/r_i) \quad (13)$$

where, ε_0 is the permittivity of the air. The capacitance values of XLPE and PP are about 0.150 and 0.198 μF/km, respectively.

3.3. Electric Field Distribution in Cable Insulation under Transient Overvoltage Conditions

Figure 10 shows the electric field of the cable under transient overvoltage conditions calculated by Equation (11). XLPE and PP cables were simulated applying transient overvoltages analyzed in Figure 9 at the rated voltages for the hot and cold cables.

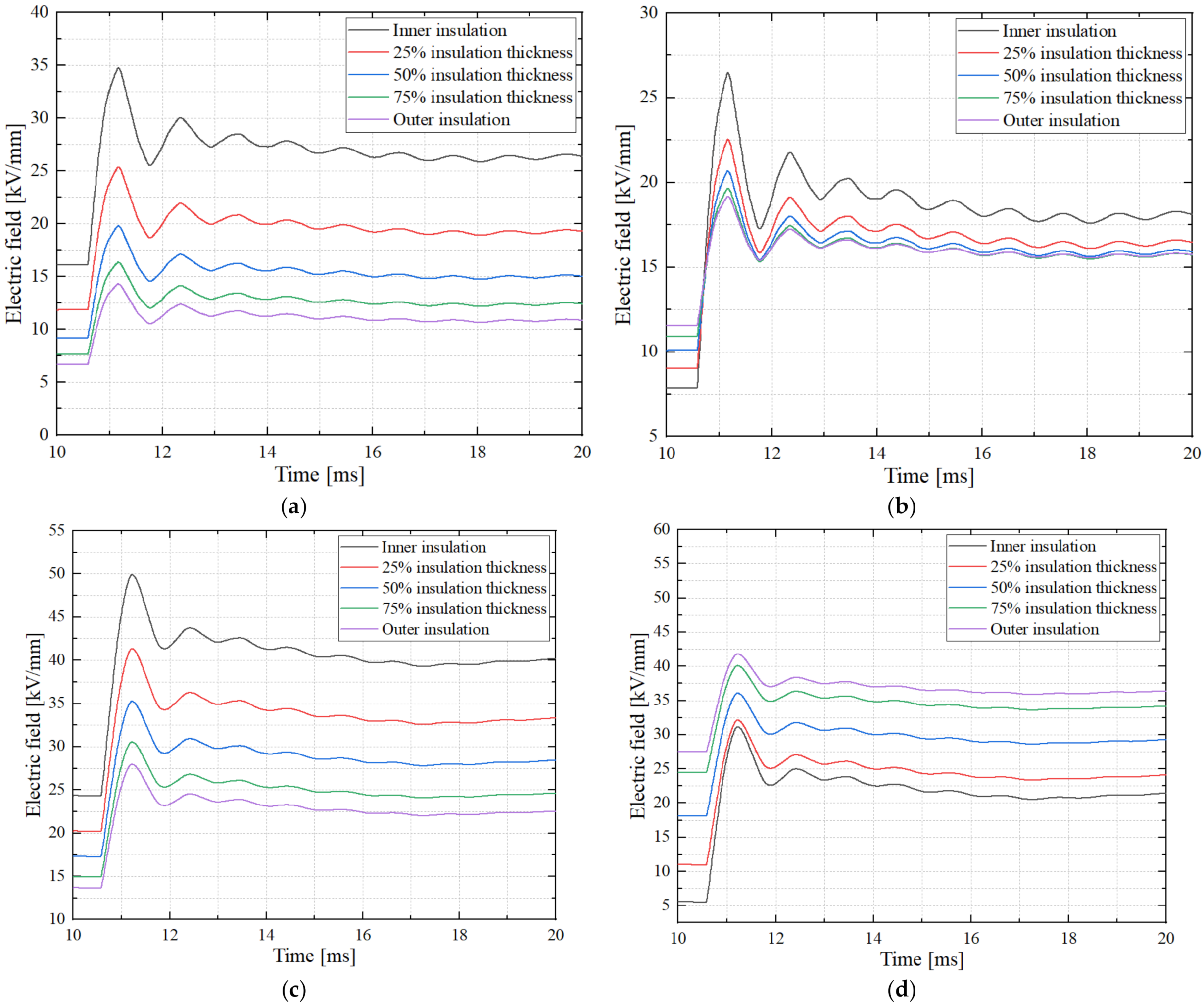

Figure 10. Electric field distribution in cable insulation under transient overvoltage conditions (**a**) XLPE cold cable; (**b**) XLPE hot cable; (**c**) PP cold cable; (**d**) PP hot cable.

Regardless of the type of insulation, higher fields were recorded in the cold cable condition, and the maximum field stress occurred in the inner insulation. In the cold cables, the electric field is prominent in the inner insulation because the electric field distribution is capacitive even before the transient state. In the case of XLPE under the hot cable condition, the electric field distribution is reversed as a transient voltage with a capacitive distribution is applied in the transient overvoltage condition. In the case of the PP cable, the maximum and minimum difference of the DC electric field in the normal state is about 25 kV/mm, which is a relatively large difference, thus the electric field is not reversed in the transient state. Since both types of cables satisfy $E(r^*) \leq E(d)$, it can be said that a stable design has been achieved.

4. Conclusions

In this paper, extruded cables for HVDC using XLPE and TP materials were designed, and their characteristics were compared and analyzed. Among various TP materials, PP material, which is in the limelight as a next-generation insulation material, was selected. The cable installation system is an MMC-HVDC with a symmetrical monopolar topology and the rated voltage and current are selected as ± 250 kV and 1 kA/pole, respectively. In order to increase the universal applicability of the research results, various cases of material properties were investigated at the design stage, and the XLPE and PP materials with typical performance were selected. As is well known, the PP insulation has better insulation performance than the XLPE, but its thermal conductivity is low. For designed cables, the PP insulation is as thin as 11 mm compared to the XLPE. The reduction in thickness leads to a reduction in the amount of insulation used as well as the cross-sectional area of the entire cable, which is economically advantageous in all processes of manufacturing, installation, and disposal. In addition, the PP has higher basic conductivity than the XLPE and no cross-linking by-products, which can reduce the electric field margin due to space charge. An increase in current capacity was also explored. At the same temperature, the ampacity of the PP is lower than that of the XLPE. However, current capacity can be increased by increasing the operating temperature in consideration of the usable temperature of the PP.

On the other hand, the thinner the insulator, the higher the field stress per unit length. The thermal conductivity of PP material varies with temperature but is about 2/3 that of the XLPE. Because of this low thermal conductivity, the ΔT between r_i and r_o is 17 °C, which is only 1.2 °C difference compared to the XLPE, despite its thinness. The temperature difference per unit length is 1.21 °C/mm, which is 1.65 times that of the XLPE. This temperature distribution greatly affects the conductivity and intensifies the imbalance of the electric field. An imbalance of electric fields can cause local aging. For overvoltages that can occur when cables are applied in HVDC systems, the maximum value of overvoltage decreases as the cable insulation becomes thinner. As such, this paper compared and analyzed XLPE and PP cables from various perspectives and concluded that PP is sufficiently attractive as a next-generation insulation material. However, at the present stage, the low thermal conductivity of PP is considered to be the most urgent problem to be solved as it is an obstacle that limits other excellent performances of PP materials.

Author Contributions: J.-I.L.; Formal analysis, J.-I.L.; Investigation, J.-I.L.; Methodology, J.-I.L. and W.-H.J.; Project administration, M.-C.D. and I.-K.Y.; Software, J.-I.L. and W.-H.J.; Supervision, M.P.; Writing—original draft, J.-I.L.; Writing—review & editing, M.-C.D. and I.-K.Y. All authors have read and agreed to the published version of the manuscript.

Funding: This research was supported by Korea Electrotechnology Research Institute (KERI) Primary research program through the National Research Council of Science & Technology (NST) funded by the Ministry of Science and ICT (MSIT) (22A01046).

Acknowledgments: This research was supported by Korea Electrotechnology Research Institute (KERI) Primary research program through the National Research Council of Science & Technology (NST) funded by the Ministry of Science and ICT (MSIT) (22A01046).

Conflicts of Interest: The authors declare no conflict of interest. The funders had no role in the design of the study.

References

1. Oni, O.E.; Davidson, I.E.; Mbangula, K.N.I. A Review of LCC-HVDC and VSC-HVDC Technologies and Applications. In Proceedings of the 2016 IEEE 16th International Conference on Environment and Electrical Engineering (EEEIC), Florence, Italy, 7–10 June 2016; pp. 1–7.
2. Flourentzou, N.; Agelidis, V.G.; Demetriades, G.D. VSC-Based HVDC Power Transmission Systems: An Overview. *IEEE Trans. Power Electron.* **2009**, *24*, 592–602. [CrossRef]

3. Wang, F.; Bertling, L.; Le, T.; Mannikoff, A.; Bergman, A. An Overview Introduction of VSC-HVDC: State-of-Art and Potential Applications in Electric Power Systems. In Proceedings of the Cigrè International Symposium, Bologna, Italy, 13–15 September 2011.
4. Bahrman, M.P.; Johnson, B.K. The ABCs of HVDC Transmission Technologies. *IEEE Power Energy Mag.* **2007**, *5*, 32–44. [CrossRef]
5. Jiang-Hafner, Y.; Duchen, H.; Karlsson, M.; Ronstrom, L.; Abrahamsson, B. HVDC with Voltage Source Converters-a Powerful Standby Black Start Facility. In Proceedings of the 2008 IEEE/PES Transmission and Distribution Conference and Exposition, Bogota, Colombia, 13–15 August 2008; pp. 1–9.
6. Ahmed, N.; Haider, A.; Van Hertem, D.; Zhang, L.; Nee, H.-P. Prospects and Challenges of Future HVDC SuperGrids with Modular Multilevel Converters. In Proceedings of the 2011 14th European Conference on Power Electronics and Applications, Birmingham, UK, 30 August–1 September 2011; pp. 1–10.
7. Bahrman, M.P. Overview of HVDC Transmission. In Proceedings of the 2006 IEEE PES Power Systems Conference and Exposition, Atlanta, GA, USA, 29 October–1 November 2006; pp. 18–23.
8. Sharifabadi, K.; Harnefors, L.; Nee, H.-P.; Norrga, S.; Teodorescu, R. *Design, Control, and Application of Modular Multilevel Converters for HVDC Transmission Systems*; John Wiley & Sons: Hoboken, NJ, USA, 2016; ISBN 1-118-85156-0.
9. Adam, G.P.; Abdelsalam, I.; Fletcher, J.E.; Burt, G.M.; Holliday, D.; Finney, S.J. New Efficient Submodule for a Modular Multilevel Converter in Multiterminal HVDC Networks. *IEEE Trans. Power Electron.* **2016**, *32*, 4258–4278. [CrossRef]
10. Elizondo, M.A.; Kirkham, H. *Economics of High Voltage Dc Networks*; Pacific Northwest National Laboratory: Richland, WA, USA, 2016.
11. Mazzanti, G.; Marzinotto, M. *Extruded Cables for High-Voltage Direct-Current Transmission: Advances in Research and Development*; Wiley-IEEE Press: Hoboken, NJ, USA, 2013.
12. Montanari, G.C.; Vaughan, A.; Morshuis, P.H.F.; Stevens, G. *Challenges and Opportunities with Interfaces and Materials for HVDC Cable Systems*; Jicable HVDC'17: Dunkerque, France, 2017.
13. Bartzsch, C.; Chakraborty, P.; Colla, L.; Fan, Y.; Fu, M.; Joubert, V.; Juvik, J.I.; Karmokar, T.; Khodabakchian, B.; Kothari, A. Surge and Extended Overvoltage Testing of HVDC Cable Systems. Systèmes de Câbles HT à Courant Continu 94. Available online: http://agp21.org/production/wp-content/uploads/2019/02/JIC-HVDC17-REE.pdf#page=12 (accessed on 10 October 2022).
14. Gustafsson, A.; Saltzer, M.; Farkas, A.; Ghorbani, H.; Quist, T.; Jeroense, M. *The New 525 KV Extruded HVDC Cable System*; ABB Grid Systems, Technical Paper; ABB: Zürich, Switzerland, 2014.
15. Bergelin, P.; Jeroense, M.; Quist, T.; Rapp, H. *640 KV Extruded HVDC Cable System*; Technical Paper; NKT: Brøndby, Denmark, 2017.
16. Kurahashi, K.; Matsuda, Y.; Ueda, A.; Demura, T.; Miyashita, Y.; Yoshino, K. The Application of Novel Polypropylene to the Insulation of Electric Power Cable. In Proceedings of the IEEE/PES Transmission and Distribution Conference and Exhibition, Yokohama, Japan, 6–10 October 2002; Volume 2, pp. 1278–1283.
17. Yoshino, K.; Ueda, A.; Demura, T.; Miyashita, Y.; Kurahashi, K.; Matsuda, Y. Property of Syndiotactic Polypropylene and Its Application to Insulation of Electric Power Cable-Property, Manufacturing and Characteristics. In Proceedings of the 7th International Conference on Properties and Applications of Dielectric Materials (Cat. No. 03CH37417), Nagoya, Japan, 1–5 June 2003; Volume 1, pp. 175–178.
18. Hosier, I.L.; Vaughan, A.S.; Swingler, S.G. An Investigation of the Potential of Polypropylene and Its Blends for Use in Recyclable High Voltage Cable Insulation Systems. *J. Mater. Sci.* **2011**, *46*, 4058–4070. [CrossRef]
19. Lee, J.-H.; Kim, S.-J.; Kwon, K.-H.; Kim, C.H.; Cho, K.C. A Study on Electrical Properties of Eco-Friendly Non-Crosslinked Polyethylene. In Proceedings of the 2012 IEEE International Conference on Condition Monitoring and Diagnosis, Bali, Indonesia, 23–27 September 2012; pp. 241–243.
20. Zha, J.-W.; Zheng, M.-S.; Li, W.-K.; Chen, G.; Dang, Z.-M. Polypropylene Insulation Materials for HVDC Cables. In *Polymer Insulation Applied for HVDC Transmission*; Springer: Berlin/Heidelberg, Germany, 2021; pp. 77–96.
21. Albertini, M.; Bareggi, A.; Caimi, L.; De Rai, L.; Dumont, A.; Bononi, S.F.; Pozzati, G.; Boffi, P. Development and High Temperature Qualification of Innovative 320 KV DC Cable with Superiorly Stable Insulation System. In Proceedings of the 9th International Conference on Insulated Power Cables, Versailles, France, 21–25 June 2015.
22. Pilgrim, J.A.; Lewin, P.L.; Vaughan, A.S. Quantifying the Operational Benefits of New HV Cable Systems in Terms of Dielectric Design Parameters. In Proceedings of the 2012 IEEE International Symposium on Electrical Insulation, San Juan, PR, USA, 10–13 June 2012; pp. 261–265.
23. Diban, B.; Mazzanti, G. The Effect of Insulation Characteristics on Thermal Instability in HVDC Extruded Cables. *Energies* **2021**, *14*, 550. [CrossRef]
24. *CIGRE WG B1.62*; Recommendations for Testing DC Extruded Cable Systems for Power Transmission at a Rated Voltage up to and Including 800 KV'. CIGRE: Paris, France, 2021. Available online: https://e-cigre.org/publication/852-recommendations-for-testing-dc-extruded-cable-systems-for-power-transmission-at-a-rated-voltage-up-to-and-including-800-kv (accessed on 10 October 2022).
25. Albertini, M.; Bononi, S.F.; Giannini, S.; Mazzanti, G.; Guerrini, N. Testing Challenges in the Development of Innovative Extruded Insulation for HVDC Cables. *IEEE Electr. Insul. Mag.* **2021**, *37*, 21–32. [CrossRef]
26. Yahyaoui, H.; Castellon, J.; Agnel, S.; Hascoat, A.; Frelin, W.; Moreau, C.; Hondaa, P.; le Roux, D.; Eriksson, V.; Andersson, C.J. Behavior of XLPE for HVDC Cables under Thermo-Electrical Stress: Experimental Study and Ageing Kinetics Proposal. *Energies* **2021**, *14*, 7344. [CrossRef]

27. *CIGRE WG B1.32*; Recommendations for Testing DC Extruded Cable Systems for Power Transmission at a Rated Voltage up to and Including 500 KV'. CIGRE: Paris, France, 2012. Available online: https://e-cigre.org/publication/496-recommendations-for-testing-dc-extruded-cable-systems-for-power-transmission-at-a-rated-voltage-up-to-500-kv-this-tb-replaces-tb-219 (accessed on 10 October 2022).
28. Mazzanti, G.; Diban, B. The Effects of Transient Overvoltages on the Reliability of HVDC Extruded Cables. Part 1: Long Temporary Overvoltages. *IEEE Trans. Power Deliv.* **2021**, *36*, 3784–3794. [CrossRef]
29. Wang, H.; Cao, J.; He, Z.; Yang, J.; Han, Z.; Chen, G. Research on Overvoltage for XLPE Cable in a Modular Multilevel Converter HVDC Transmission System. *IEEE Trans. Power Deliv.* **2016**, *31*, 683–692. [CrossRef]
30. Zhou, Y.; Yuan, C.; Li, C.; Meng, P.; Hu, J.; Li, Q.; He, J. Temperature Dependent Electrical Properties of Thermoplastic Polypropylene Nanocomposites for HVDC Cable Insulation. *IEEE Trans. Dielect. Electr. Insul.* **2019**, *26*, 1596–1604. [CrossRef]
31. Meng, P.; Zhou, Y.; Yuan, C.; Li, Q.; Liu, J.; Wang, H.; Hu, J.; He, J. Comparisons of Different Polypropylene Copolymers as Potential Recyclable HVDC Cable Insulation Materials. *IEEE Trans. Dielect. Electr. Insul.* **2019**, *26*, 674–680. [CrossRef]
32. Huang, X.; Fan, Y.; Zhang, J.; Jiang, P. Polypropylene Based Thermoplastic Polymers for Potential Recyclable HVDC Cable Insulation Applications. *IEEE Trans. Dielect. Electr. Insul.* **2017**, *24*, 1446–1456. [CrossRef]
33. Vahedy, V. Polymer Insulated High Voltage Cables. *IEEE Electr. Insul. Mag.* **2006**, *22*, 13–18. [CrossRef]
34. Brakelmann, H.; Anders, G.J. Current Rating Considerations in Designing HVDC Cable Installations. *IEEE Trans. Power Deliv.* **2018**, *33*, 2315–2323. [CrossRef]
35. Hampton, R.N. Feature Article—Some of the Considerations for Materials Operating under High-Voltage, Direct- Current Stresses. *IEEE Electr. Insul. Mag.* **2008**, *24*, 5–13. [CrossRef]
36. Montanari, G.C.; Seri, P.; Lei, X.; Ye, H.; Zhuang, Q.; Morshuis, P.; Stevens, G.; Vaughan, A. Next Generation Polymeric High Voltage Direct Current Cables—A Quantum Leap Needed? *IEEE Electr. Insul. Mag.* **2018**, *34*, 24–31. [CrossRef]
37. Roy, M.; Nelson, J.K.; MacCrone, R.K.; Schadler, L.S. Candidate Mechanisms Controlling the Electrical Characteristics of Silica/XLPE Nanodielectrics. *J. Mater. Sci.* **2007**, *42*, 3789–3799. [CrossRef]
38. Vaughan, A.S.; Green, C.D.; Hosier, I.L.; Stevens, G.C.; Pye, A.; Thomas, J.L.; Sutton, S.J.; Geussens, T. Thermoplastic High Performance Cable Insulation Systems for Flexible System Operation. In Proceedings of the 2015 IEEE Electrical Insulation Conference (EIC), Seattle, WA, USA, 7–10 June 2015; pp. 543–546.
39. Li, Z.L.; Fan, M.S.; Zhou, S.F.; Du, B.X. BNNS Encapsulated TiO_2 Nanofillers Endow Polypropylene Cable Insulation with Enhanced Dielectric Performance. *IEEE Trans. Dielect. Electr. Insul.* **2021**, *28*, 1238–1246. [CrossRef]
40. Du, B.X.; Han, C.; Li, J.; Li, Z. Temperature-Dependent DC Conductivity and Space Charge Distribution of XLPE/GO Nanocomposites for HVDC Cable Insulation. *IEEE Trans. Dielect. Electr. Insul.* **2020**, *27*, 418–426. [CrossRef]
41. Hu, S.; Zhang, W.; Wang, W.; Li, J.; Shao, Q.; Zhang, Y.; Zhang, Q.; Huang, S.; Hu, J.; Li, Q.; et al. Comprehensive Comparisons of Grafting-Modified Different Polypropylene as HVDC Cable Insulation Material. *IEEE Trans. Dielect. Electr. Insul.* **2022**, *29*, 1865–1872. [CrossRef]
42. Du, B.X.; Hou, Z.H.; Li, Z.L.; Li, J. Temperature Dependent Space Charge and Breakdown Strength of PP/ULDPE/Graphene Nanocomposites for HVDC Extruded Cable Insulation. *IEEE Trans. Dielect. Electr. Insul.* **2019**, *26*, 876–884. [CrossRef]
43. Cao, L.; Zhong, L.; Li, Y.; Gao, J.; Chen, G. Crosslinking Dependence of Direct Current Breakdown Performance for XLPE-PS Composites at Different Temperatures. *Polymers* **2021**, *13*, 219. [CrossRef]
44. Wang, Y.; Wang, C.; Xiao, K. Investigation of the Electrical Properties of XLPE/SiC Nanocomposites. *Polym. Test.* **2016**, *50*, 145–151. [CrossRef]
45. Enhanced Electrical Properties of Styrene-Grafted Polypropylene Insulation for Bulk Power Transmission HVDC Cable. *CSEE JPES* **2022**. [CrossRef]
46. Lin, X.; Siew, W.H.; Liggat, J.; Given, M.; He, J. Octavinyl Polyhedral Oligomeric Silsesquioxane on Tailoring the DC Electrical Characteristics of Polypropylene. *High Voltage* **2022**, *7*, 137–146. [CrossRef]
47. Cao, W.; Li, Z.; Sheng, G.; Jiang, X. Insulating Property of Polypropylene Nanocomposites Filled with Nano-MgO of Different Concentration. *IEEE Trans. Dielect. Electr. Insul.* **2017**, *24*, 1430–1437. [CrossRef]
48. Li, G.; Zhou, X.; Li, X.; Wei, Y.; Hao, C.; Li, S.; Lei, Q. DC Breakdown Characteristics of XLPE/BNNS Nanocomposites Considering BN Nanosheet Concentration, Space Charge and Temperature. *High Voltage* **2020**, *5*, 280–286. [CrossRef]
49. Zhang, X.; Fujii, M. Measurements of the Thermal Conductivity and Thermal Diffusivity of Polymers. *Polym. Eng. Sci.* **2003**, *43*, 1755–1764. [CrossRef]
50. Lee, H.B.; Lee, B.C.; Kim, J.H.; Nam, Y.H.; Kang, J.W. Improvement of the Conductor Temperature Calculation Algo-Rithm for Calculating the Allowable Current in the Underground Channel. *Trans. Korean Inst. Electr. Eng.* **2018**, *67*, 352–357.
51. Green, C.; Vaughan, A.; Stevens, G.; Pye, A.; Sutton, S.; Geussens, T.; Fairhurst, M. Thermoplastic Cable Insulation Comprising a Blend of Isotactic Polypropylene and a Propylene-Ethylene Copolymer. *IEEE Trans. Dielect. Electr. Insul.* **2015**, *22*, 639–648. [CrossRef]
52. Ouyang, Y. *Novel Thermoplastic Material Concepts for High Voltage Cable Insulation*; Chalmers University of Technology: Gothenburg, Sweden, 2021.
53. Boggs, S.; Damon, D.H.; Hjerrild, J.; Holboll, J.T.; Henriksen, M. Effect of Insulation Properties on the Field Grading of Solid Dielectric DC Cable. *IEEE Trans. Power Deliv.* **2001**, *16*, 456–461. [CrossRef]

54. Jeroense, M.J.P.; Morshuis, P.H.F. Electric Fields in HVDC Paper-Insulated Cables. *IEEE Trans. Dielect. Electr. Insul.* **1998**, *5*, 225–236. [CrossRef]
55. Jeroense, M.J.P. *Charges and Discharges in HVDC Cables—In Particular in Impregnated HVDC Cables*; Delft University of Technology, Delft University Press: Delft, The Netherlands, 1997.
56. COMSOL Multiphysics®. *COMSOL Multiphysics Version 5.5*; COMSOL AB: Stockholm, Sweden, 2019.
57. Goertz, M.; Wenig, S.; Beckler, S.; Hirsching, C.; Suriyah, M.; Leibfried, T. Analysis of Cable Overvoltages in Symmetrical Monopolar and Rigid Bipolar HVDC Configuration. *IEEE Trans. Power Deliv.* **2020**, *35*, 2097–2107. [CrossRef]
58. Jardini, J.A.; Vasquez-Arnez, R.L.; Bassini, M.T.; Horita, M.A.; Saiki, G.Y.; Cavalheiro, M.R. Overvoltage Assessment of Point-to-Point vsc-Based Hvdc Systems. *Przegląd Elektrotechniczny* **2015**, *91*, 105–112. [CrossRef]
59. Palone, F.; Marzinotto, M.; Buono, L. Temporary Overvoltage Mitigation in Symmetrical Monopole VSC-MMC HVDC Links. In Proceedings of the 2017 AEIT International Annual Conference, Cagliari, Italy, 20–22 September 2017; pp. 1–6.
60. Mazzanti, G.; Seri, P.; Diban, B.; Stagni, S. Preliminary Experimental Investigation of the Effect of Long Temporary Overvoltages on the Reliability of HVDC Extruded Cables. In Proceedings of the 2020 IEEE 3rd International Conference on Dielectrics (ICD), Valencia, Spain, 5 July 2020; pp. 49–52.
61. Ghorbani, H.; Jeroense, M.; Olsson, C.-O.; Saltzer, M. HVDC Cable Systems—Highlighting Extruded Technology. *IEEE Trans. Power Deliv.* **2014**, *29*, 414–421. [CrossRef]
62. *CIGRE WG B4.57*; Guide for the Development of Models for HVDC Converters in a HVDC Grid. CIGRE: Paris, France, 2014. Available online: https://e-cigre.org/publication/604-guide-for-the-development-of-models-for-hvdc-converters-in-a-hvdc-grid (accessed on 10 October 2022).
63. Manitoba HVDC Research Centre. *PSCAD Version 4.6.3.0*; Windows NT 6.2; Manitoba Hydro International Ltd.: Winnipeg, MB, Canada, 2018.